RPC Background Studies at CMS Experiment

Abdurrahman Abdullah Al-Mashad
(abdurrahman.muhammed@cern.ch)

Supervised by: Dr. **Mohammed Attia Mahmoud**
(mohammed.attia@cern.ch)

Francesco Carnevali
(francesco.carnevali@cern.ch)

13 June 2022 - 5 August 2022

Abstract

The Resistive Plate Chambers (RPCs) are employed in the CMS Experiment at the LHC as dedicated trigger system both in the barrel and in the endcap. This report presents the measurements of the Background rate in the RPC considering the LHC fulling scheme.

Contents

0.1 Resistive Plate Chambers

The Compact Muon Solenoid (CMS) Muon system, designed to trigger and identify muons, is based on three different technologies in Run-1 and Run-2; Drift Tube (DT) in the barrel region, Cathode Strip Chamber (CSC) in the endcap and Resistive Plate Chambers (RPC) in both the barrel and endcap, as shown in Figure 1. For muon triggering purposes, the CMS trigger is staged in two levels. The Level-1 Trigger (L1) [1] which is hardware based and uses information of the muon system exclusively, and the High Level Trigger (HLT) [2] which is software based and combines information from muon system and inner tracker to identify muons.

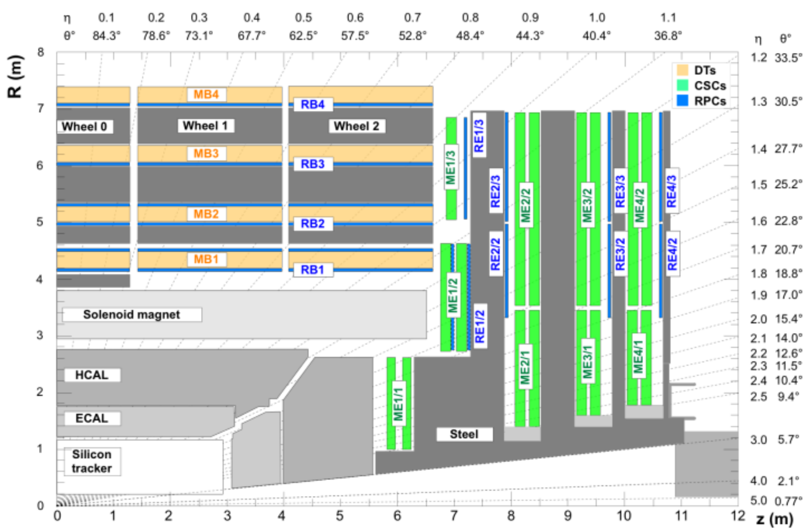

Figure 1: Cross section of a quadrant of the CMS detector. Taken from [3].

The Resistive Plate Chambers (RPCs) are particle detectors that use a sensitive medium in the form of gas to detect charged particles. They are widely used in high-energy physics experiments (ALICE, ATLAS and CMS) for its good intrinsic efficiency, long-term stability and large sensitive area for detection. Furthermore, RPCs have a fast response with a time resolution of few nanoseconds. An RPC detector consists of two parallel high resistive plates (typically phenolic resins and glass) of few mm thickness, separated by a small gas gap.

0.1.1 Detector Design and Principle Work

RPCs have a very simple design, a gas detecting volume is enclosed by two resistive electrodes which are made from Bakelite with a resistivity of 10^{10} – 10^{12} Ωcm and have conducting coating (usually graphite). Rectangular plastic frames are used for electrodes mounting, and small plastic separators keep the constant distance between them, thus ensuring electrical and mechanical stability. The inside surface of the gaps is coated with a 35 – 45 μm linseed oil [4] in order to smoothen the surface and quench the Ultraviolet (UV) photons [5]. The outer surfaces of the gaps are coated with conductive graphite paint, thus forming the High Voltage (HV) and ground electrodes as shown in Figure 2(a).

As RPCs are gaseous detectors, their working principle is based on the ionization effect in the gas, caused by a charged particle passing through the detector volume. The avalanche multiplication is caused by a cluster of electrons obtained after the ionization [6]. This leads to an electron charge developed inside the gap, which further drifts towards the anode. The useful signal of the detector is the charge induced on the pickup electrode. The HV power supply is compensating the charge collected on the electrodes as shown in Figure 2(b).

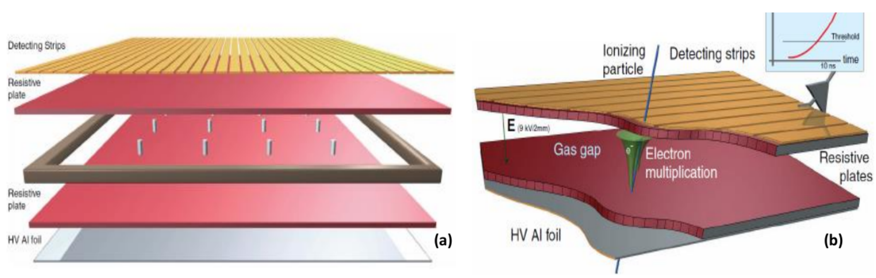

Figure 2: (a) Schematic view of the different layers of an RPC. (b) Illustration of the RPC detecting principle.

In the CMS detector the RPC system consists of 1,056 double-gap chambers operating in avalanche mode [7]. The two gaps are placed one on top of another with a common readout performed by copper readout strips placed in between and isolated from the graphite by mylar sheets as shown in Figure 3.

The standard RPC gas mixture is composed of the three components listed below:

- 95.2 % $C_2H_2F_2$, acting as the charge carrier gas [8].
- 4.5 % iC_4H_{10}, acting as a quencher gas to absorb UV photons from molecule de-excitation.
- 0.3 % SF_6, control the excess electrons through its high electron affinity [9].

The gas mixture is kept at 21°C and 35 % – 40 % humidity is added in order to maintain the bakelite resistivity, which increases as the bakelite dries out [10].

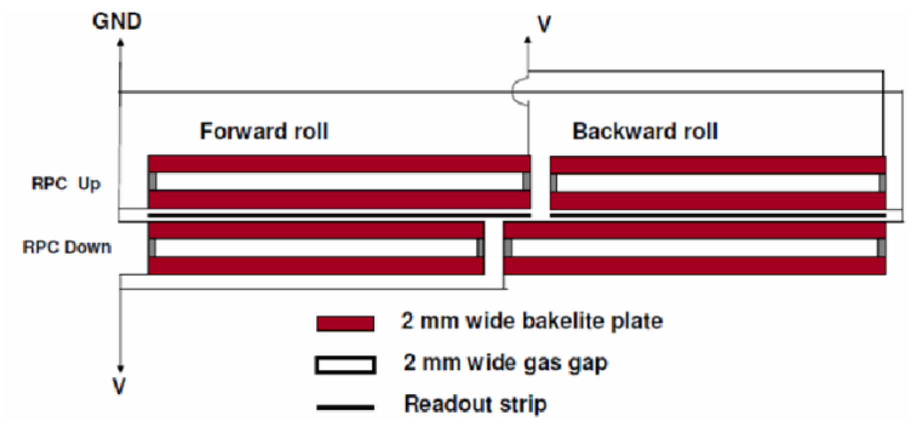

Figure 3: Schematic view of RPC double-gap design.

0.1.2 Detector Layout

In the CMS detector the need to trigger on the transverse momentum p_T of passing muons is the main purpose behind the detector layout of the RPC system. The p_T is measured with the bending of the muon in the CMS magnetic field and this requires a muon to cross at least 3 out of 4 layers in the Muon system.

The RPC system is divided into two regions following the CMS experiment configuration which are: barrel region and endcap region. It is composed of 1056 chambers covering a pseudorapidity range of $|\eta| < 1.2$ in the barrel and $0.9 < |\eta| < 1.9$ in the endcap. It has more than 110,000 electronic channels and covers a sensitive area of 3,500 m^2.

Barrel Region

The barrel system consists of 480 RPCs, distributed equally among 5 wheels along the beam pipe (Wheel 0, Wheel ±1, Wheel ±2). As shown in Figure 4, each wheel consists of 4 stations (RB1, RB2, RB3 and RB4) with increasing radius R, which are interleaved with the steel return yoke. Each wheel is divided into 12 sectors (S01-S12), as dictated by the mechanical construction of the CMS return yoke. Due to mechanical reasons, RB3 and RB4 are further divided to + and − along ϕ in all sectors apart from S04, S09 and S11 in RB4. Since RB4/S09 and RB4/S11 are in the feet of the barrel wheel, they consist of only a single RPC chamber. RB4/S04 is divided even more along 4 chambers (++, +, −, − −).

Further to the trigger requirements, the chambers are divided with respect to pseudorapidity in 2 partitions, called rolls (forward and backward). Only RB2in in Wheels -1, 0, +1 and RB2out in Wheels -2, +2 are divided in 3 rolls (forward, middle and backward) [11].

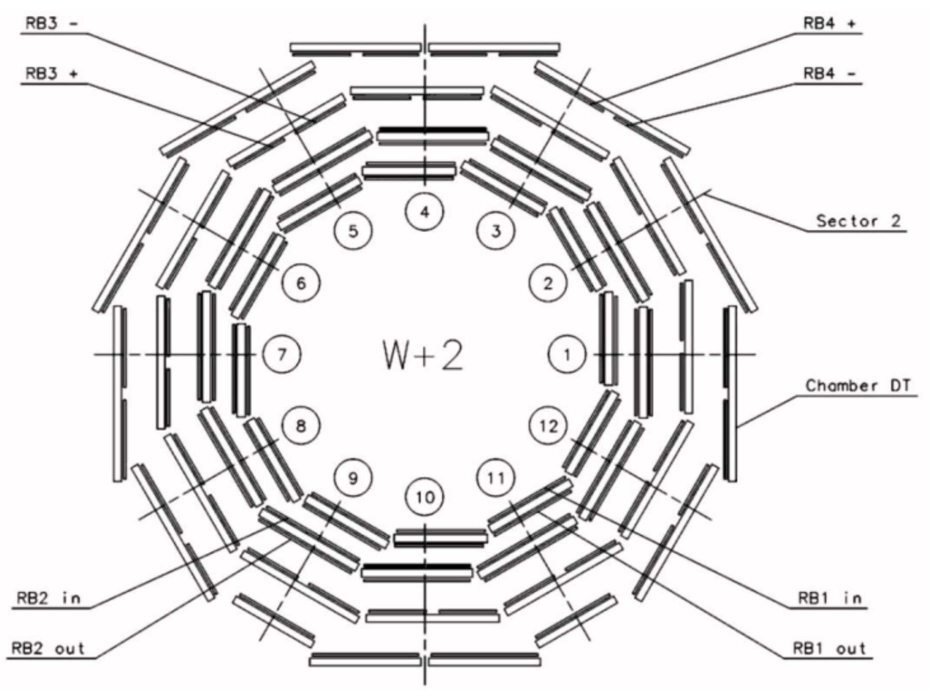

Figure 4: Sketch of one of the 5 barrel wheels with its numbered sectors.

Endcap Region

The design in the endcap is very similar to the one used in the barrel. The main difference comes from the geometry aspects and the fine segmentation which higher multiplicity in the forward regions require.

The endcap system consists of 576 RPCs, which are distributed along 8 disks named RE ±1, RE ±2, RE ±3 and RE ±4 [4 disks per each endcap (positive and negative)], as shown in Figure 5. Each disk is divided into 36 sectors along ϕ, and has two concentric rings [ring 2 (R2) and ring 3 (R3)]. There are 36 10° trapezoidal RPC chambers building up each ring, which are further divided into three rolls, labeled A, B and C with respect to increasing η. Each chamber is indicated as a segment CH01 through CH36 within a ring. Segment CH01 lays on the positive X-axis direction and the numbering proceeds anti-clockwise in respect to the interaction point.

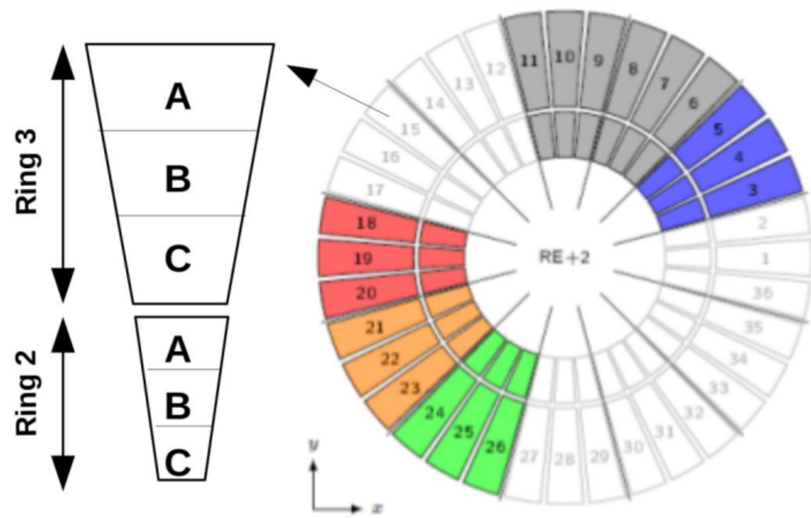

Figure 5: Sketch of one of the endcap disks with its numbered sectors.

0.2 RPC Background Studies

We use the CMS experimental data from the LHC Run-2 (2015–2018) in order to evaluate the radiation background in the CMS RPC system, and use it to get the offline analysis.

0.3 Results

This is the offline data which is stored in big events, and this data takes a lot of memory, that is why it is required to extract from them only the collection that is needed for the analysis and store them as a hit-tree. RPC reads the experimental data in 6 windows which called BXs, every window has 25 ns. From the other side the LHC BX ID has a clock, a BXs of colliding, and the BXs of not colliding.

There are three different chambers in the barrel region that has been studied in this project. The first chamber is W-2/RB1in/S04 with the condition (region=0, ring=-2, station=1, layer=1, sector=4), the second chamber is W0/RB2out/S10 with the condition of (region=0, ring=0, station=2, layer=2, sector=10) and finally the third chamber is W+1/RB4/S02 with the condition (region=0, ring=+1, station=4, sector=2) with constant luminosity = 12 $\times 10^{33}$ $cm^{-2}.s^{-1}$.

These are the plots for the there different chambers which have been already explained in the previous paragraph. These plots are the distribution of the number of RPC clusters. The RPC readout in 6 windows which vary between $[-2 \ldots 3]$, the RPC hits read in this windows are clusterized in order to form clusters and this clusters are assigned with corresponding BX ID. The LHC BX ID full scheme is ordered in a logical way following 25 ns and every one of them is called LHC BX.

Shown in Figure 6, is the rate of RPC BX Vs LHC BX ID. So, the LHC BX ID scheme includes colliding and not colliding BX.

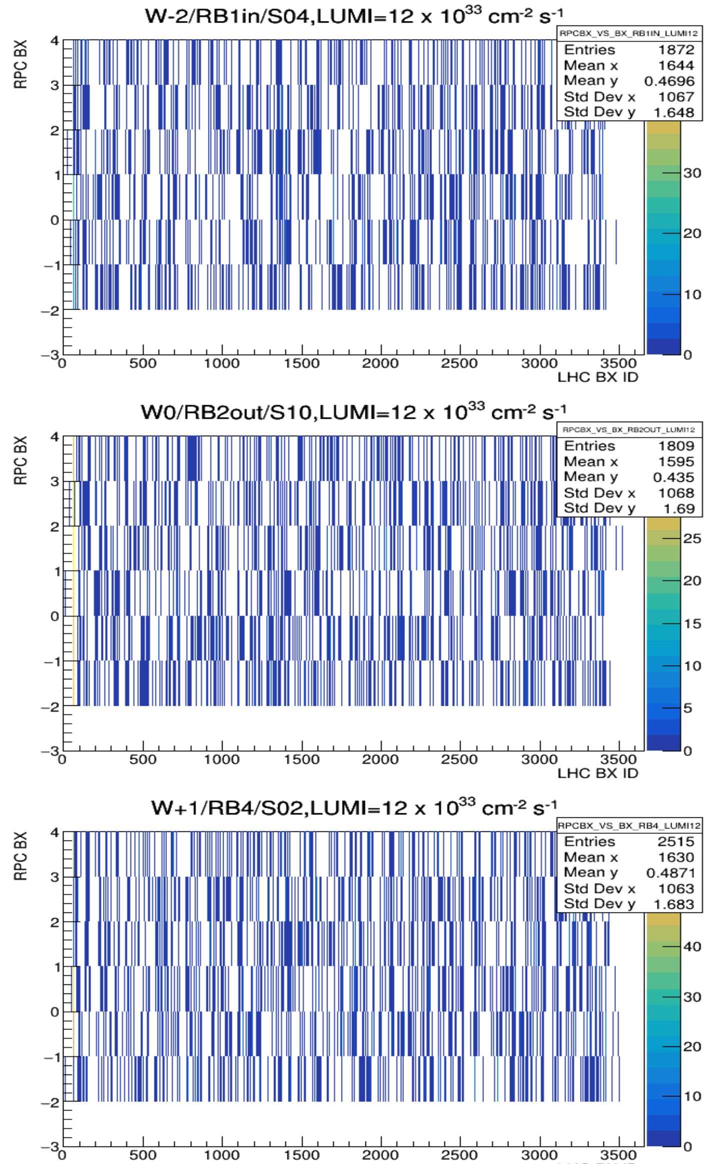

Figure 6: The relation between the RPC BX vs LHS BX ID for three different chambers in the barrel region (W-2/RB1in/S04, W0/RB2out/S10 and W+1/RB4/S02), respectively.

In Figure 7, these plots are the projection in the X-axis, which counts the number of hits per BX ID considering all RPC BX. The peak at first is the first colliding BX at LHC BX ID = 62. If more events occurred, the number of hits will increase.

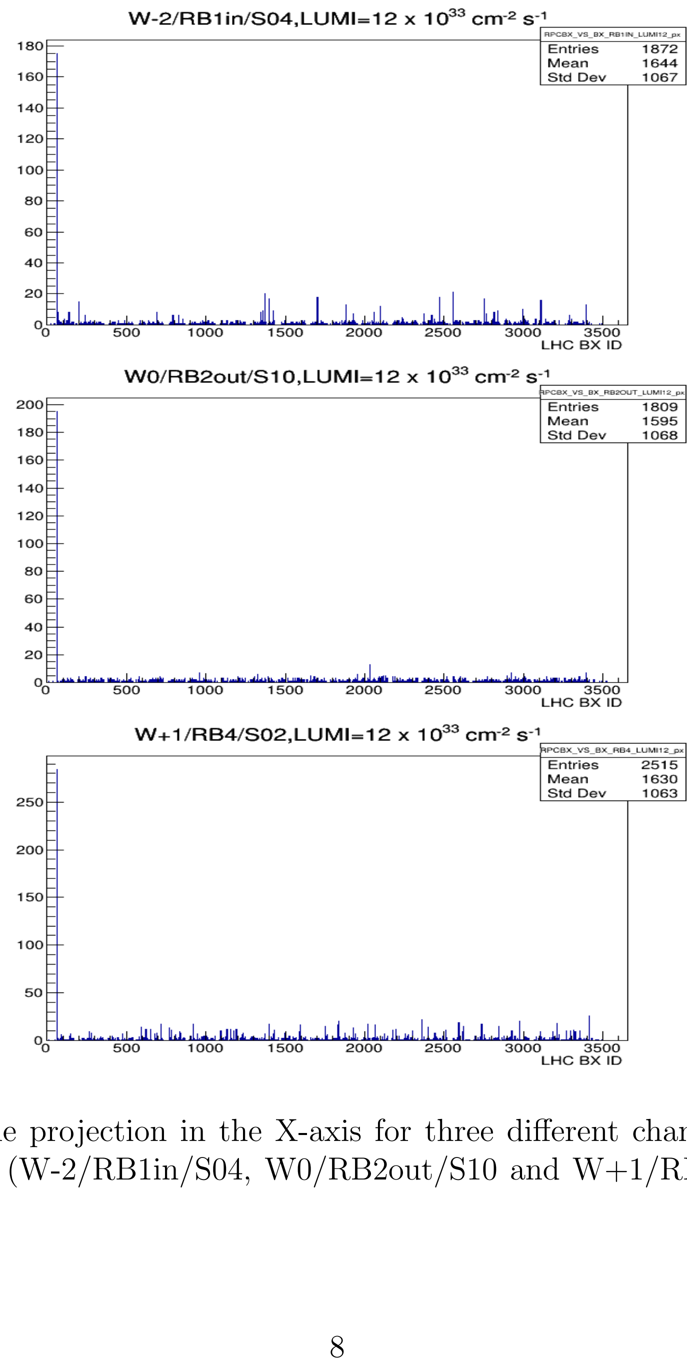

Figure 7: The projection in the X-axis for three different chambers in the barrel region (W-2/RB1in/S04, W0/RB2out/S10 and W+1/RB4/S02), respectively.

Shown in Figure 8, is the zoom view of Figure 7 in the range between 1,000 to 2,000 in the X-axis. As shown that the rate vary, but it is required to do a correct map between the RPC readout windows and LHC BX ID which is taken into account in the last set of Figure 9.

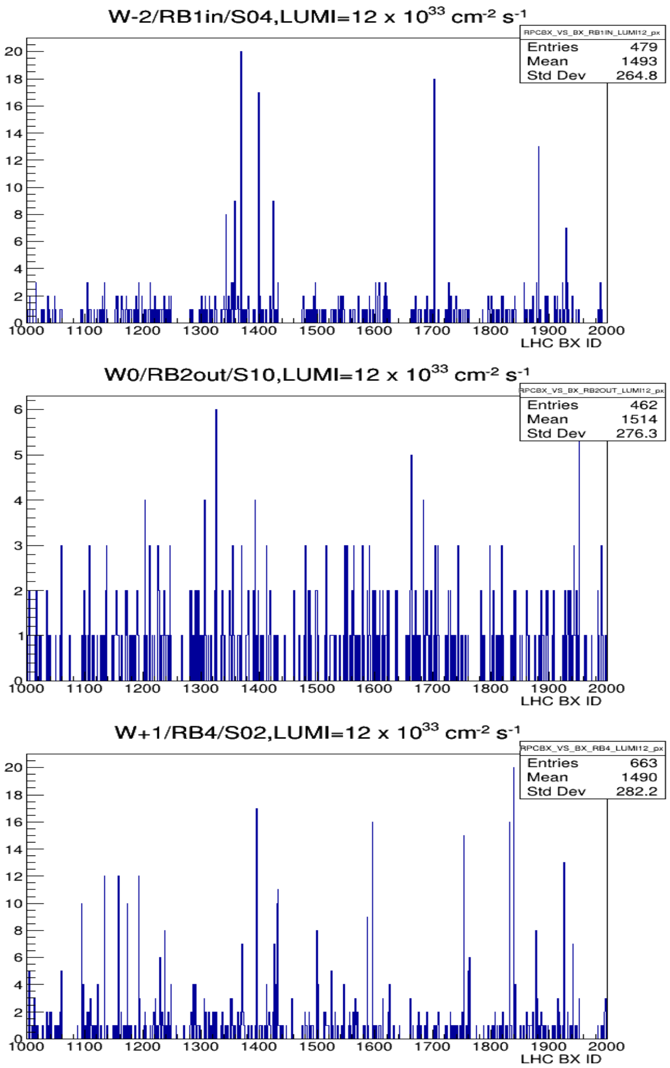

Figure 8: The projection in the X-axis in the range between 1,000 and 2,000 for three different chambers in the barrel region (W-2/RB1in/S04, W0/RB2out/S10 and W+1/RB4/S02).

In Figure 9, this is the clear plots which show how the rate is bigger where there are colliding BXs, and how the rate is lower where there are not colliding BXs.

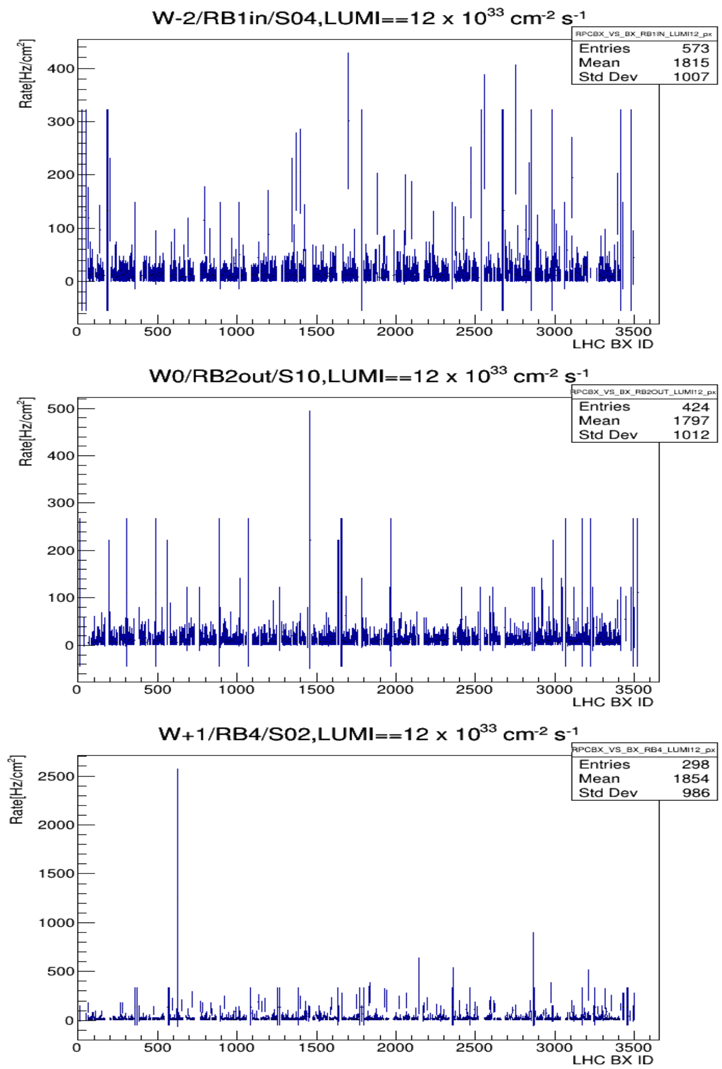

Figure 9: The rate of RPC background for three different chambers in the barrel region (W-2/RB1in/S04, W0/RB2out/S10 and W+1/RB4/S02).

0.4 Conclusion

This is a part of a bigger study which the data is evaluated, the background rate depends on the full scheme, when there are collisions the rate is higher while it is low when there are not collisions.

List of Figures

Bibliography

[1] CMS Collaboration. The TriDAS project, technical design report. Volume 1: The level-1 trigger, CERN-LHCC-2000-038, http://cdsweb.cern.ch/record/706847.

[2] CMS Collaboration. The TriDAS project, technical design report. Volume 2: Data acquisition and high-level trigger technical design report, CERN-LHCC-2002-026, http://cdsweb.cern.ch/record/578006.

[3] Serguei Chatrchyan et al. The Performance of the CMS Muon Detector in Proton-Proton Collisions at $\sqrt{s} = 7$ TeV at the LHC. JINST, 8:P11002, 2013.

[4] M. Abbrescia et al. Effect of the Linseed Oil Treatment on the Performance of the Resistive Plate Counters. Tech. Rep. CMS-NOTE-1997-018.

[5] L. Changguo. RPC electrode material study. Nucl. Instrum. Meth. A, 602(3):761–765, 2009.

[6] M. Abbrescia et al. The simulation of resistive plate chambers in avalanche mode: Charge spectra and efficiency. Nucl. Instrum. Meth. A, 431:413–427, 1999.

[7] CMS Collaboration. CMS Physics Technical Design Report. Vol. I: Detector Performance and Software, CERN/LHC, 1, 2006.

[8] M. Abbrescia et al. Properties of the $C_2H_2F_4$ based gas mixture for avalanche mode operation of Resistive Plate Chambers. Tech. Rep. CMS-NOTE-1997-004, CERN, Geneva, Jan 1997.

[9] P. Camarri et al. Streamer suppression with SF_6 in RPCs operated in avalanche mode. Nucl. Instrum. Meth. A, 414:317–324, 1998.

[10] M. Abbrescia et al. Study of long-term performance of CMS RPC under irradiation at the CERN GIF. Nucl. Instrum. Meth. A, 533:102–106, 2004.

[11] CMS Collaboration. The Muon Project, CMS Technical Design Report. CERN/LHCC 97-32, CMS-TDR-003, 1997.